REVIEW ARTICLE

Three-dimensional visualization and quantification for the growth and invasion of oral squamous cell carcinoma

Yoshihito Shimazu, Tomoo Kudo, Hisao Yagishita, Takaaki Aoba*

Department of Pathology, Nippon Dental University School of Life Dentistry at Tokyo, 1-9-20 Fujimi, Chiyoda-ku, Tokyo 102-8159, Japan

Summary Recent advance in three-dimensional (3D) imaging technology allows us to inspect visually and quantitatively the architecture of complex biological tissues and pathological lesions. We initiated histology-based 3D reconstruction of oral squamous cell carcinoma (SCC) in order to collect quantitative information of diagnostic value regarding cancer invasion and prognosis. The basic procedures for 3D reconstruction are: preparation of serial histological sections in combination with immunostaining of cell/tissue constituents of interest, alignment and superposition of digitized images, computer-assisted color segmentation of labeled targets, and finally viewing and morphometric analysis of the reconstruct. Our past experience showed that cytokeratin-positive tumor parenchyma can be segmented readily from the surrounding stroma with the aid of Image-J and RATOC TRI-SRF2 software. Cytoplasm/nucleus segmentation of individual SCC cells was also feasible at higher magnifications, leading to quantitative analysis of several histological parameters in tissue space, e.g., parenchyma and stroma volume, nuclear numbers and nuclear/cytoplasm volume ratio, as well as proliferation activity of cancer cells by counting separately the number of Ki-67 positive and negative nuclei in the parenchyma. The results support the wide potential usage and advantage of histology-based 3D reconstruction in cancer biology understanding and pathological diagnosis.
© 2009 Japanese Association for Dental Science. Published by Elsevier Ireland. All rights reserved.

Contents

* Corresponding author. Tel.: +81 3 3261 8899; fax: +81 3 3261 8969.
  E-mail address: patho-aoba@tokyo.ndu.ac.jp (T. Aoba).

1. Introduction

About 90% of cancers originate from epithelial tissue. Organs such as the skin and oral—pharyngeal mucosa are continuously exposed to environmental insults, so that squamous cell carcinoma (SCC) is the primary tumor type in head and neck cancer. At present, head and neck SCCs hold the seventh position in the worldwide cancer statistics, largely as a consequence of abundant tobacco smoking and alcohol consumption in industrialized countries [1,2]. Although potentially curable by local radiotherapy and surgical resection, the overall 5-year survival rate of the malignant tumors is only 50%, largely because of the propensity of some tumors to disseminate via the lymphatics to regional lymph nodes [3]. Hence, there is an urgent need to identify characteristics of the primary tumor that might predict nodal metastasis.

It is now clear that cancer arises through a multistep, mutagenic process whereby cancer cells acquire a common set of properties including unlimited proliferation potential, self-sufficiency in growth signals, and resistance to antiproliferative and apoptotic signals [4—7]. In addition to the genetic background of cancer cells, much attention is now directed to the interactive nature and outcome between tumor cells and host stromal cells, on the basis of supposition that host stromal cells profoundly influence many steps of tumor progression, such as tumor cell proliferation, invasion, angiogenesis, metastasis, and even malignant transformation [8—11]. Pathologists routinely examine tumor growth and invasion progressing in a complex microenvironment that is regulated by both tumor cells and host stromal cells, making diagnosis regarding their origin, malignancy and prognostic prospects. In such conventional pathological diagnosis even with serial sections of a good quality, it is difficult, if not impossible, to grasp the three-dimensional (3D) structure of cancer lesions in a complex microenvironment under a microscope. In this sense, 3D histomorphometric parameters regarding tumor alveolar structure and spatial distribution of cancer foci in a microenvironment will be of inexpensive value in prediction and diagnosis of tumor aggressiveness and malignancy.

Recent advance in 3D imaging technology allows us to inspect the details of tumor architecture [12—15]. In the past few years, we initiated to reconstruct SCC architectures at the invasion front using serial histological sections and, on that basis, to document growth and invasion patterns of SCC. In this communication, we aimed to overview the current status of histology-based 3D reconstruction by showing an example of visualization of SCC arising on the lateral border of the tongue. The use of archival human tissues in this study was performed in accordance with the Declaration of Helsinki and was approved by the Institutional Review Board of the Nippon Dental University.

2. How to reconstruct a 3D architecture of squamous cell carcinoma

The common procedures for histological 3D reconstruction are: preparation of paraffin-embedded tissue specimens, staining or labeling of serially cut sections with specific markers depending on the nature and properties of targets of interest, alignment of the serial sectional images (i.e., image registration), automated segmentation of the labeled structure(s), and viewing and morphometric analysis of the reconstruct [16]. In the literature, several techniques for automated 3D reconstruction using paraffin-embedded histological sections have been documented [12,17—19], but each of the 3D reconstruction procedures, particularly the distortion-free image registration, yet remained as major challenges. An alternative approach to circumvent the use of serially cut sections is the reconstruction of certain tissue components (e.g., blood vessels in a stromal space) by means of laser scanning confocal microscopy (LSCM) from a single, thick, paraffin-embedded tissue sample [20]. Introduction of LSCM makes use of optical sections, eliminating the need for image registration. However, due to optical limitations this technique is usually limited to 50—100 μm thick tissue fragments [21]. Moreover, Lin et al. [19] pointed out that the use of a thick paraffin-embedded section for LSCM observation, instead of serially cut sections with the intention to avoid heterogeneous distortions from section to section, may bring about uneven penetration of antibodies into the thick paraffin-embedded tumor region, making it difficult to discriminate between the absence of a signal and a lack of complete penetration of the antibody of interest. Another method to avoid image distortion caused by physically cutting sections is by using the cut face of a tissue block for image registration, instead of the resulting sections themselves [22]. In this technique, gross structures with the intrinsic color or autofluorescence can be captured and registered in a semi-automated manner, but a major drawback is the limitation of applying extrinsic labelings for specific visualization of microscopic structures of interest [13]. In contrast, the use of serial histological sections has the great advantage that immunohistochemical staining can be applied on archival, paraffin-embedded material for recognition of cells and tissue components in the same way as pathologists routinely examine under light microscopy.

In the following paragraphs, we explain briefly the basic procedure of 3D reconstruction we have developed using paraffin-embedded, serially cut histological sections in combination with dual immunostaining to facilitate recognition of multiple components in tumor lesions.

2.1. Preparation of consecutive histological sections and immunostaining

A case of SCC shown in Fig. 1A was selected from the archives of the Surgical Pathology Laboratory, Nippon Dental University Hospital. Tissue specimens were fixed in 10% formaldehyde and sectioning of paraffin blocks for 3D reconstruction was performed on an electronic, motorized, rotary microtome (Microm HM 355S, MICROM International GmbH, Walldorf, Germany). One critical technical point was the use of a tissue-array apparatus (Azumaya, Model KIM-1, Japan) yielding a tissue core biopsy of 3 mm in diameter (Fig. 1B and C), which made it possible to obtain constantly 200–600 serial sections with equal thickness and minimal distortion of sections from regions of interest. As described later, the preparation of uniform, circular sections much helped to save time and efforts in recording digital images and subsequent computation steps for image registration. Visualization of multiple components was usually performed by dual immunohistochemical staining using the avidin–biotin-complex that can highlight the structural features of interest in a combination of discrete colors. For instance, in order to visualize the proliferation activity of cancer cells in SCC, the cytokeratin-positive tumor parenchyma was stained using diaminobenzidine tetrahydrochloride (DAB), while the Ki-67 positive nuclei were discriminated using Vector Blue. In order to improve the signal to noise ratio during image acquisition, no counterstaining was used in this case.

2.2. Image acquisition and registration

Red–green–blue (RGB) color images of consecutive serial sections were acquired using a CCD camera (AxioCam MRC, Carl Zeiss, Germany), attached to a conventional transmitted light microscope (Eclipse E600, NIKON, Japan). For securing high spatial resolution, histological images were acquired using a 10-times objective and stored as 32 bit RGB TIFF format (size 1388×1040 pixels). When using the CCD camera, it was necessary to align carefully the targeted histological objects with a rotating microscope stage. Practically, individual microscopic fields in series were set as closely as possible in the same position by comparing a live color image of the section under examination with contours of the already captured profiles in an overlay display. It is notable that the outcome of image registration alignment of consecutive serial sections depends to the utmost extent on the performance of this 'rough' initial alignment that can correct mainly for shifts and rotations of sections on the glass slides.
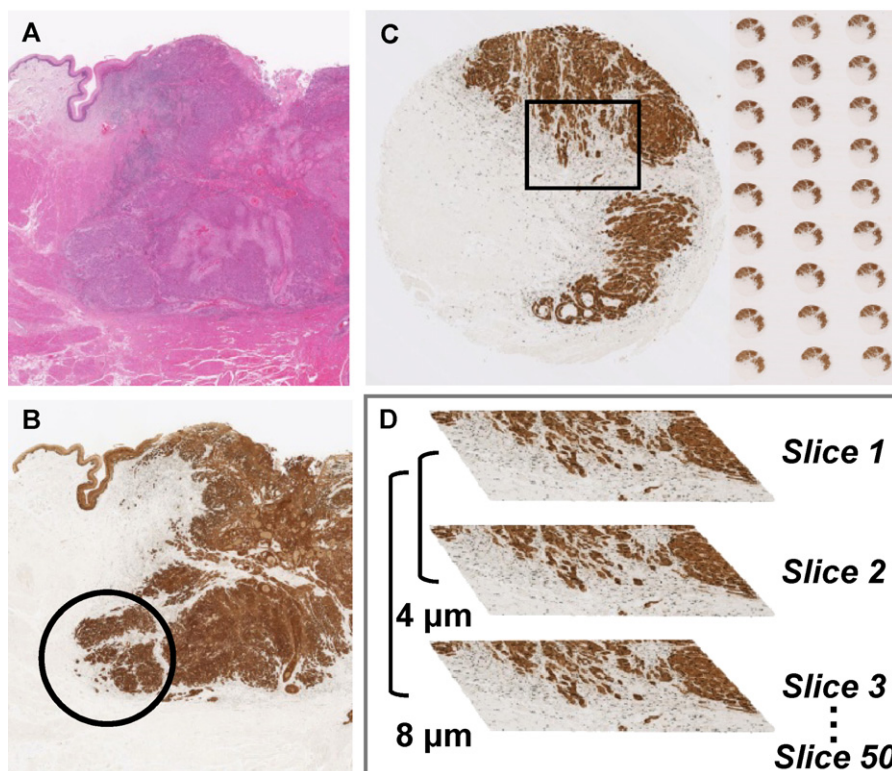
Figure 1   (A) Microphotograph of a case of tongue squamous cell carcinoma with hematoxylin and eosin staining. (B) Immunostaining of a consecutive section with a cocktail of cytokeratin antibodies, i.e., AE1/AE3, 34βE12 and MNF116. A tissue core biopsy of 3 mm in diameter, as shown circle, was dissected out of the deepest invasion front using a tissue-array apparatus. (C) Preparation of serial sections (4 μm thick) from the core specimen and subsequently their immunostaining using cytokeratin and Ki-67 antibodies. The region of tumor invasion front, indicated by a frame, was captured for 3D reconstruction with a CCD camera. (D) Alignment of serially captured images in the z-direction.

At present, we also utilize a virtual microscope (NanoZoomer RS, Hamamatsu Photonics, Japan), which provides a great advantage of automated, high-speed and high-resolution digitization of consecutive images in series.

After storage of an entire series of digitized images, the computer-assisted image registration was executed for more accurate, fine-tune alignment, including correction for shifts, rotations and stretching in *x* and *y* direction (Fig. 1D). To this purpose, we have used both open-source Image-J (http://rsb.info.nih.gav/ij/downlood.html) and commercially available TRI-SRF2 (Ratoc System Eng. Co., Japan) software. It is notable that Image-J is efficient and highly useful for 3D alignment of multiple consecutive circular images, which were recorded from the tissue-array specimens, without specific reference points corresponding to the fiducially marker. In some cases of image registration, however, we experienced the failure of conversion in computation using Image-J, so that we needed the introduction of reference points with the aid of TRI-SRF2.

3. Three-dimensional reconstruction of SCC at the invasion front

The architecture of SCC in general becomes more irregular and complex with increasing malignancy. In the literature, much effort has been given to assess invasion patterns on microscopic slides with reference to pathologic and clinical data [23–27]. To date, several investigators [23,28,29] documented malignancy grading systems based on the characteristics of the deep invasive front area of oral SCC, but controversies yet continue as to what criteria with respect to the invasive front characteristics of oral SCC is indeed of prognostic value [30,31]. The microscopic features of cancer lesions are usually assessed in two-dimensional (2D) histological slides, but the actual shape and configuration of microscopic structures cannot be extrapolated on the basis of examination of histological sections alone. Of particular importance in pathological diagnosis, an anastomosing network of tumor strands in tissue volume may appear in 2D sections as discontinuous segments of small foci. The nature of continuity or sequestration of cancer cells certainly reflects their biological propensity or malignancy. In the following paragraphs, we present an example of the 3D feature of SCC at the deepest invasion front.

3.1. Segmentation of cancer cells and nuclei

Microscopic examination of the SCC case with hematoxylin–eosin staining showed that the cancer lesion expanded and invaded into tongue muscle with moderate peritumoral inflammation (Fig. 1A). To detect and delineate tumor parenchyma from inflammatory cell infiltrating stroma, we performed immunohistochemistry using cytokeratin antibodies. One practical problem encountered for segmentation of tumor parenchyma from the surrounding stroma was the heterogeneous properties of cancer cells with respect to their cytokeratin expression. We first screened with a variety of anti-cytokeratin antibodies and, based on their adequate selective and intensive immunoreactivity for tumor cells, we used a cocktail of three antibodies, i.e., AE1/AE3, 34βE12 and MNF116, for the current 3D reconstruction. Immunostaining with the cocktailed antibodies proved that DAB colored cancer parenchyma yielded high contrast sufficiently enough to demarcate the parenchyma–stroma margin by means of the automated RGB color-gradient segmentation without any operator-dependent subjectivity such as drawing by hand of the presumed parenchyma–stroma borderline. Following the labeling of the parenchyma region, the stroma was isolated by subtracting the parenchyma region from the whole tissue volume with the aid of computation logics of inversion/subtraction procedure on the basis of the binary gray levels. According to the same computation logics, both Ki-67-positive and negative nuclei embedded within the cytokeratin-positive cancer cytoplasm were segmented autonomously. In this segmentation of nuclei, we adopted one criterion that all binary objects assigned as nuclei should have connection between two consecutive images, while all binary signals in an image without connection with corresponding objects in adjacent images should be deleted as noise signals. The results of segmentation for each microscopic field were validated by overlaying segmented elements in the original immunostained section on a computer screen.

3.2. 3D visualization of SCC tumor architecture

Fig. 2 stems from an image stack of 50 serial sections of 4 μm thickness that focus on the invasion front of SCC as shown in Fig. 1. On 2D views, it was not easy to make diagnosis on whether individual cancer foci were in a form of continuing strands or islands but, on 3D view, it was verified that cancer parenchyma (Fig. 2A) comprised of interconnected strands and resulted in finger-like infiltration into the stroma (Fig. 2B). In addition to visual inspection, application of the computation logics, i.e., the labeling/erosion/dilation of the segmented 3D data, helps to validate the continuity of tumor parenchyma and, if any, to assess quantitatively the number, size and spatial distance of individual cancer foci that are circumscribed separately in the stroma. We call this image processing as "virtual microanatomy" of cancer architectures. In this case of SCC, this image processing indeed validated the continuity of cancer parenchyma in the reconstructed region. According to the documented invasive front grading of SCC, four patterns of cancer invasion based on 2D view were postulated: (1) pushing, well delineated infiltrating borders, (2) infiltrating, solid cords, bands and/or strands, (3) small groups or cords of infiltrating cells, and (4) marked and widespread cellular dissociation in small groups and/or in single cells [28,29]. In our case of SCC, 2D view support grade (3) but, on the available 3D view, it may be appropriate to assign it into grade (2). Obviously, taking into the loco-regional heterogeneity of cancer cells, it is needed to scrutinize three-dimensionally over a wider invasive front and larger tissue volume for making concrete diagnosis. Superposition of Ki-67 positive and negative nuclei onto the parenchymal space provided evidence for the high cellular density and high proliferation activity of cancer cells (Fig. 2C and D). Remarkably, Ki-67 positive nuclei aligned preferentially along the parenchyma–stroma margin and at the tip of finger-like infiltration into the stroma. The polarization of high mitotic activity supports the theory that most aggressive cells reside in the deepest invasive front of the tumor [29].
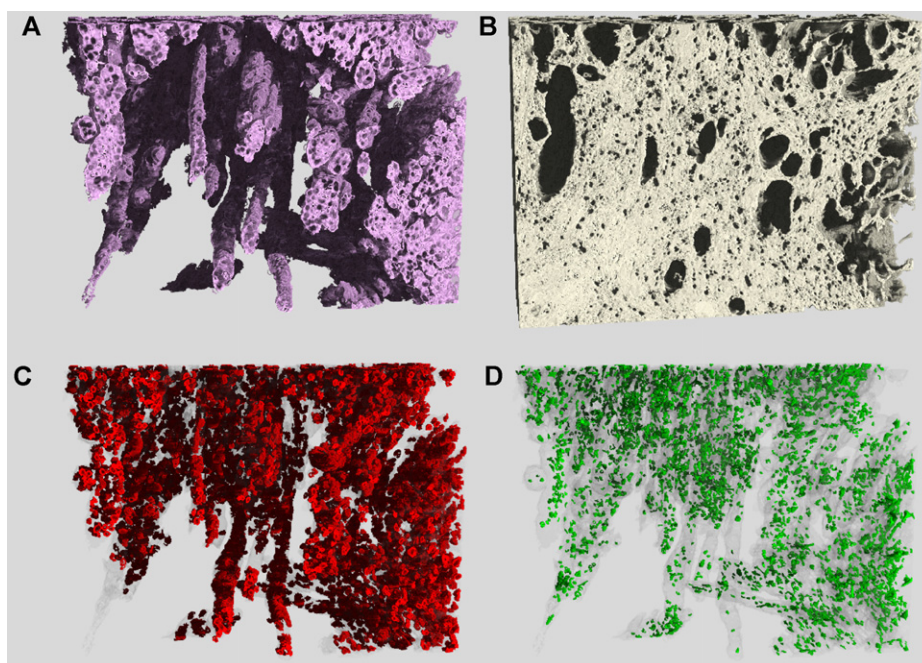
Figure 2 (A) 3D viewing of the segmented tumor parenchyma comprising the interconnected strands of cancer cells. (B) The segmented stroma leaving the holes corresponding to the parenchyma. (C) Superposition of Ki-67 positive nuclei on the parenchyma. (D) Superposition of Ki-67 negative nuclei. The segments of cells and nuclei were visualized in 3D using a polygonal approximation of the object surfaces. Note the higher density of Ki-67 positive nuclei, indicative of high proliferation activity.

3.3. Morphometric analysis of cancer cells

A great advantage of 3D analysis of tumor architecture is the capability of quantification over thousands or more of cells and nuclei, improving the reliability of diagnosis-useful parameters. Quantitative data obtained from the reconstructed SCC at the invasion front were: within an overall reconstructed tissue volume of $2.96 \times 10^8 \ \mu m^3$, the tumor parenchyma filled $0.77 \times 10^8 \ \mu m^3$, while the stroma with blood and lymphatic vessels and infiltrating cells corresponded to another $2.19 \times 10^8 \ \mu m^3$. Within the parenchyma region, the nucleus—cytoplasm (N/C) volume ratio was about 0.12 and the total number of nuclei assigned for both Ki-67 positive and negative amounted to 5748 and 3484, respectively, indicating that the proliferation activity of cancer cells at the invasion front, expressed by the ratio of Ki-67 positive nuclei/total nuclei, was 62%. Our recent experiments proved that the utilization of virtual microscopy for image acquisition improves markedly the quality of recorded digitized images, particularly their spatial and RGB color resolution, that is essential to the accuracy and precision of 3D visualization and quantification.

4. Perspective of 3D reconstruction approach in relation to oral cancer biology and diagnosis

A better understanding of the mechanisms underlying progression and invasion/metastasis of oral cancer is essential to improve prognosis prediction and treatment modalities, because it is of great concern that little improvement in 5-year survival rate of sufferers have been achieved over the last 25 years [1—3,23—29]. Current treatment regimes are guided at least in part by traditional clinico-pathologic factors such as TNM stage, histological grade and patient age. Recent research endeavor has been directed to the tissue specificity of carcinoma—stroma interactions that most likely accounts for a tissue- and cell-type specific role of the microenvironment in carcinoma development [8—11]. Tumor microenvironment includes extracellular matrix, blood vasculature, inflammatory cells and fibroblasts (Fig. 3). These considerations support the importance of novel diagnostic scheme and modalities that are based on the spatial organization of carcinoma in the coherent microenvironment. In this respect, the histology-based 3D reconstruction of SCC is undoubtedly useful for understanding of tumor parenchyma—stroma interactions and regional distribution of multiple tissue constituents. As described in the preceding paragraphs, the principle and laboratory procedure of 3D reconstruction we developed are applicable on serial sections of a variety of tissues and structures. At present, the potential of the histology-based 3D reconstruction is mainly limited by the availability of unequivocal cellular and molecular markers that specifically visualize the object(s) of interest by immunohistochemistry or other techniques. In light of the recent innovation and advances of automated instrumentation and technology in the field of surgical pathology as described later, we believe that in the coming few years, 3D examination of tumor specimens is becoming a common practice in cancer research and histopathologic diagnosis, specifically regarding tumor-associated angiogenesis and lymphangiogenesis.
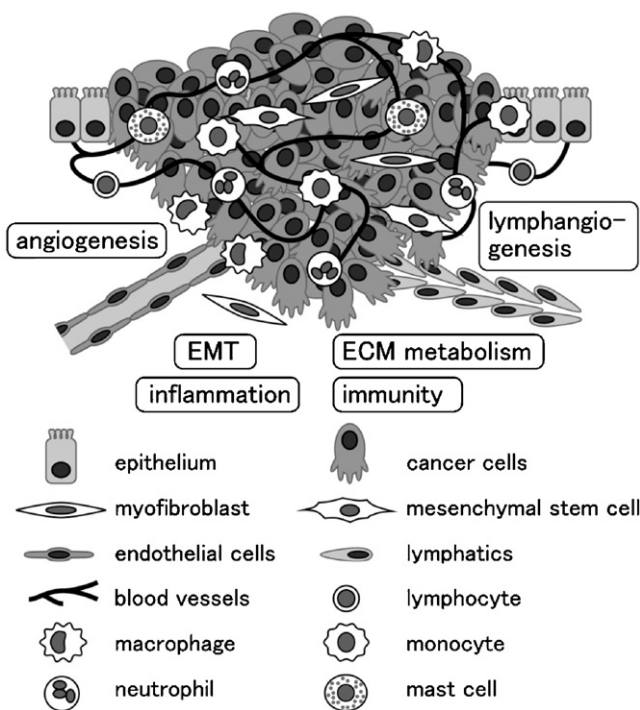
Figure 3 Schematic illustration of tumor microenvironment and cell/tissue features of potential value in understanding cancer biology and clinical prognosis. EMT, epithelial mesenchymal transformation; ECM, extracellular matrices.

4.1. Visualization of a network of blood vessels in solid tumors

The most promising field for 3D investigation is the microvascular architecture in normal and pathological tissue. Angiogenesis, one of the critical steps required for solid tumors to grow beyond their dormant state [32], relies on the formation of new blood vessels by endothelial cells through either the sprouting or intussusception (i.e., the division of vessels by transluminal invagination and pillar formation) of parent blood vessels [33]. Many steps are required to convert endothelial sprouts into functional, blood-carrying vessels. The term "maturation" describes the stepwise transition from an actively growing vascular bed to a quiescent, fully formed and functional network: the recruitment of pericytes, the deposition of ECM proteins into the subendothelial basement membrane and the reduced endothelial cell proliferation promote vessel maturation [10,34]. The literature documented that blood vascular maturation is frequently compromised in many tumors, the vasculature of which are leaky and inefficient at oxygen delivery [35—37]. Of most interest, recent work [38,39] emerged a new theory that "normalizing" blood vessels to better perfuse the tumor tissue may actually down-regulate the signaling pathways that contribute to tumor growth and that a change in endothelial shape, even without alterations in vessel numbers, suffices to induce a shift to reduced malignancy and metastasis. According to this theory, it is becoming critical to elucidate phenotypic heterogeneity of endothelial cells within blood vessels indicative of their proper development and function [40]. Our seminal work using virtual microscopy proved the feasibility of employing simultaneously multiple antibodies against blood vessel endothelial and mural cells, such as CD31, CD34, CD105 and α-SMA, for 3D visualization of vessel wall components expressing different markers. From a patho-diagnostic point of view, it has long been recognized that intra- and peritumor microvessel densities are valuable prognostic parameters [41]. To date, however, microvessel density measurements in association with SCC and other oral tumors yet remain to be accomplished. Collectively, the loco-regional 3D analysis of a network of tumor-blood vessels with characterization of their vessel walls is an urgent task to validate the hypothesis that the endothelial normalization indeed blocks tumor invasion and metastasis in oral cancers.

4.2. Lymphangiogenesis and lymphnode metastasis

Recently, lymphangiogenesis is becoming a hot topic of embryonic development and carcinogenesis in accordance with the discovery of specific molecular markers of lymphatic endothelium, such as LYVE-1, podoplanin or D2-40 [42—44]. For many types of carcinoma including oral SCC, lymph node involvement is associated with poor survival and the presence of lymph node metastasis often represents an early prognostic indicator of cancer invasiveness and metastatic dissemination [45—49]. Taking into account the potential prognostic value of lymphangiogenesis in patients with cancer, systematic efforts have been initiated to organize discussion on the standardization of the immunohistochemical method for lymphangiogenesis assessment and to establish a quantification method that is characterized by a low intra- and inter-observer variability [50]. We also have preliminary evidence that a combination of antibodies CD31 and D2-40 is appropriate for discrimination of blood and lymphatic

endothelial cells in the microenvironment surrounding SCC at the invasion front. Several studies have shown that the density of lymphatic vessels located immediately adjacent to the tumor is associated with the presence of lymph node metastases [48,49], but there is still a debate about the role of intratumorous versus peritumorous lymphatic vessels in the pathology of primary human tumors [51]. In relation to the mechanism of how to establish intratumorous lymphatics, it is not known whether this is achieved through the formation and invasion of new lymphatics within the tumor, i.e., tumor lymphangiogenesis, or by expansion and invasion of preexisting lymphatics at the tumor periphery [52]. An intriguing hypothesis is that the infiltration of lymphatic vessels into the tumor parenchyma might establish a paracrine signalling pathway for tumor cell growth and invasion through the release of specific growth factors or chemokines, rather than having a passive role in cancer metastasis by creating an increased opportunity for metastatic tumor cells to leave the primary tumor site. In the same vein as mentioned about tumor angiogenesis, it is becoming a realistic task to gain quantitative information about the architecture of blood and lymphatic vessels, e.g., vessel volume and surface area, vessel diameter, and node and terminal branch counts within region of interest.

4.3. Routine use of 3D reconstruction in research and surgical pathology laboratories

The phenotypic features and structures of certain tumor classification vary between patients and even from region to region within a tumor case. By recognizing diverse histological features of pathologic human tissues, pathologists wait a long while to have at hand a computer-assisted histomorphometric system that much help to minimize the subjective nature of assessment of various histological and cytological features. Recent innovation of an automated sectioning apparatus (AS-200/AS-2005, Kurabo, Japan) can save substantially a time consuming and laborious effort needed for the physical preparation of a large number of consecutive histological sections. Immunolabeling of the resulting sections also can be conducted efficiently with the aid of an automated immunostaining apparatus that is widely used in surgical pathology laboratories. As mentioned above, the utilization of virtual microscopy makes it possible to conduct efficiently the image acquisition and registration procedure. At present, various types of image processing software are available from multiple sources; some of the operator-driven computation steps including color segmentation of targets of interest and noise deletion may not be familiar enough for many potent users to execute the computation procedure by themselves, but it is not a huge obstacle for software providers to develop a menu-driven and user-oriented formulation on users' demand. Taken together, it is feasible to note that the potential of introducing histology-based 3D reconstruction in both research purposes and surgical pathology application is growing considerably. In biological and clinical oncology, measurements of tumor properties, such as location, infiltration pattern, metastasis, and angiogenesis-related vascular patterns obtained from diagnostic images are a standard method of monitoring patient response to anticancer therapies [15,36,37,39,44]. Most likely, the histology-based 3D recon-

struction will become a future *in vivo* analysis of invasion and metastasis of cancer cells and of new therapy and treatment regimen targeting cancer cells.

5. Conclusive remarks

Our recent experience supports the feasibility and potential of histology-based 3D reconstruction of oral cancers in order to unveil a complexity of tumor architecture and associated interaction of multiple tissue and cell constituents in tissue volume. In studies of 3D reconstruction, segmentation of targeted constituents in the tissue space is a key advantage. Our current experimental protocol using dual immmunostaining with cytokeratin and Ki-67 antibodies is convenient to segregate tumor parenchyma from the surrounding stroma and to assess quantitatively the proliferation activity of tumor cells in a computation-dependent manner without any operator-biased manipulation. To date, we have focused attention on tumor invasion front by collecting a 3D spectrum of invasion patterns of SCC arising at tongue. The histological features of SCC may differ widely from area to area within the same tumor, so that 3D analysis of tumor structures in a wider region and at higher spatial resolution is required. Along this line of consideration, we now continue collection of 3D data by utilizing virtual microscopy as mentioned above. This stage of our project is still in its infancy but we feel confident that histological 3D data of oral cancers will lead to establishment of prognostic criteria for cancer malignancy based on the cancer cells—microenvironment interaction.

Acknowledgements

References

[1] Ziober BL, Silverman SS, Kramer RH. Adhesive mechanisms regulating invasion and metastasis in oral cancer. Crit Rev Oral Biol Med 2001;12:499—510.

[2] Pentenero M, Gandolfo S, Carrozzo M. Importance of tumor thickness and depth of invasion in nodal involvement and prognosis of oral squamous cell carcinoma: a review of the literature. Head Neck 2005;27:1080—91.

[3] Kademani D. Oral cancer. Mayo Clin Proc 2007;82:878—87.

[4] Christofori G. New signals from the invasive front. Nature 2006;441:444—50.

[5] Joyce JA, Pollard JW. Microenvironmental regulation of metastasis. Nat Rev Cancer 2009;9:239—52.

[6] Polyak K, Weinberg RA. Transitions between epithelial and mesenchymal states: acquisition of malignant and stem cell traits. Nat Rev Cancer 2009;9:2652—3273.

[7] Califano J, van der Riet P, Westra W, Nawroz H, Clayman G, Piantadosi S, et al. Genetic progression model for head and neck

cancer: implications for field cancerization. Cancer Res 1996;56:2488–92.

[8] Hinz B, Phan SH, Thannickal VJ, Galli A, Bochaton-Piallat ML, Gabbiani G. The myofibroblast: one function, multiple origins. Am J Pathol 2007;170:1807–16.

[9] Bhowmick NA, Neilson EG, Moses HL. Stromal fibroblasts in cancer initiation and progression. Nature 2004;432:332–7.

[10] Jain RK. Molecular regulation of vessel maturation. Nat Med 2003;9:685–93.

[11] Luo J, Solimini NL, Elledge SJ. Principles of cancer therapy: oncogene and non-oncogene addiction. Cell 2009;136:823–37.

[12] Braumann UD, Kuska JP, Einenkel J, Horn LC, Loffler M, Hockel M. Three-dimensional reconstruction and quantification of cervical carcinoma invasion fronts from histological serial sections. IEEE Trans Med Imaging 2005;24:1286–307.

[13] Gijtenbeek JMM, Wesseling P, Maass C, Burgers L, van der Laak JAWM. Three-dimensional reconstruction of tumor microvasculature: simultaneous visualization of multiple components in paraffin-embedded tissue. Angiogenesis 2005;8:297–305.

[14] Wentzensen N, Braumann UD, Einenkel J, Horn LC, Doeberitz MK, Loffler M, et al. Combined serial section-based 3D reconstruction of cervical carcinoma invasion using H&E/p16INK4a/CD3 alternate staining. Cytometry A 2007;71A:327–33.

[15] Fukumura D, Jain RK. Imaging angiogenesis and the microenvironment. APMIS 2008;116:695–715.

[16] Shimazu Y, Aoba T, editors. Three-dimensional motion view of tissue architectures and lesions. Tokyo: Ishiyaku Pub.; 2009 [in Japanese].

[17] Kay PA, Robb RA, Bostwick DG. Prostate cancer microvessels: a novel method for three-dimensional reconstruction and analysis. Prostate 1998;37:270–7.

[18] Einenkel J, Kuska JP, Horn LC, Wentzensen N, Hockel M, Braumann UD. Combined three-dimensional microscopic visualisation of tumour-invasion front of cervical carcinoma. Lancet Oncol 2006;7:698.

[19] Lin A, Ai Z, Lee SC, Bajcsy P, Péer J, Leach L, et al. Comparing vasculogenic mimicry with endothelial cell lined vessels: techniques for 3D reconstruction and quantitative analysis of tissue components from archival paraffin blocks. Appl Immunohistochem Mol Morphol 2007;15:113–9.

[20] Dickie R, Bachoo RM, Rupnick MA, Dallabrida SM, DeLoid GM, Lai J, et al. Three-dimensional visualization of microvessel architecture of whole-mount tissue by confocal microscopy. Microvasc Res 2006;72:20–6.

[21] Hossler FE, Douglas JE. Vascular corrosion casting: review of advantages and limitations in the application of some simple quantitative methods. Microsc Microanal 2001;7:253–64.

[22] Weninger WJ, Mohun T. Phenotyping transgenic embryos: a rapid 3-D screening method based on episcopic fluorescence image capturing. Nat Genetics 2002;30:59–65.

[23] Yamamoto E, Kohama G, Sunagawa H. Mode of invasion: bleomycin sensitivity, and clinical course in squamous cell carcinoma of the oral cavity. Cancer 1983;51:2175–80.

[24] Crissman JD, Liu WY, Gluckman JL, Cummings G. Prognostic value of histopathologic parameters in squamous cell carcinoma of the oropharynx. Cancer 1984;54:2995–3001.

[25] Asakage T, Yokose T, Mukai K, Tsugane S, Tsubono Y, Asai M, et al. Tumor thickness predicts cervical metastasis in patients with stage I/II carcinoma of the tongue. Cancer 1998;82:1443–8.

[26] Sheahan P, O'Keane C, Sheahan JN, O'Dwyer TP. Predictors of survival in early oral cancer. Otolaryngol Head Neck Surg 2003;129:571–6.

[27] Keski-Säntti H, Atula T, Törnwall J, Koivunen P, Mäkitie A. Elective neck treatment versus observation in patients with T1/T2 N0 squamous cell carcinoma of oral tongue. Oral Oncol 2006;42:96–101.

[28] Bryne M, Koppang HS, Lilleng R, Kjaerheim A. Malignancy grading of the deep invasive margins of oral squamous cell

carcinomas has high prognostic value. J Pathol 1992;166:375–81.

[29] Woolgar JA. Histopathological prognosticators in oral and oropharyngeal squamous cell carcinoma. Oral Oncol 2006;42:229–39.

[30] Bryne M. Is the invasive front of an oral carcinoma the most important area for prognostication? Oral Dis 1998;4:70–7.

[31] Sawair FA, Irwin CR, Gordon DJ, Leonard AG, Stephenson M, Napier SS. Invasive front grading: reliability and usefulness in the management of oral squamous cell carcinoma. J Oral Pathol Med 2003;32:1–9.

[32] Folkman J. Angiogenesis in cancer, vascular, rheumatoid and other disease. Nat Med 1995;1:27–31.

[33] Jubb AM, Oates AJ, Holden S, Koeppen H. Predicting benefit from anti-angiogenic agents in malignancy. Nat Rev Cancer 2007;S5–14.

[34] Eberhard A, Kahlert S, Goede V, Hemmerlein B, Plate KH, Augustin HG. Heterogeneity of angiogenesis and blood vessel maturation in human tumours: implications for antiangiogenic tumour therapies. Cancer Res 2000;60:1388–93.

[35] Tozer GM, Kanthou C, Baguley BC. Disrupting tumour blood vessels. Nat Rev Cancer 2005;5:423–35.

[36] Ribatti D, Nico B, Crivellato E, Vacca A. The structure of the vascular network of tumors. Cancer Lett 2007;248:18–23.

[37] Adams RH, Alitalo K. Molecular regulation of angiogenesis and lymphangiogenesis. Nat Rev Mol Cell Biol 2007;8:464–78.

[38] Jain RK. Normalization of tumor vasculature: an emerging concept in antiangiogenic therapy. Science 2005;307:58–62.

[39] Mazzone M, Dettori D, Leite de Oliveira R, Loges S, Schmidt T, Jonckx B, et al. Heterozygous deficiency of PHD2 restores tumor oxygenation and inhibits metastasis via endothelial normalization. Cell 2009;136:839–51.

[40] Bautch VL. Endothelial cells form a phalanx to block tumor metastasis. Cell 2009;136:810–2.

[41] Weidner N. Intratumor microvessel density as a prognostic factor in cancer. Am J Pathol 1995;147:9–19.

[42] Kahn HJ, Bailey D, Marks A. Monoclonal antibody D2-40, a new marker of lymphatic endothelium, reacts with Kaposi's sarcoma and a subset of angiosarcomas. Mod Pathol 2002;15:434–40.

[43] Evangelou E, Kyzas PA, Trikalinos TA. Comparison of the diagnostic accuracy of lymphatic endothelium markers: Bayesian approach. Mod Pathol 2005;18:1490–7.

[44] Baluk P, McDonald DM. Markers for microscopic imaging of lymphangiogenesis and angiogenesis. Ann NY Acad Sci 2008;1131:1–12.

[45] Beasley NJP, Prevo R, Banerji S, Leek RD, Moore J, van Trappen P, et al. Intratumoral lymphangiogenesis and lymph node metastasis in head and neck cancer. Cancer Res 2002;62:1315–20.

[46] Franchi A, Gallo O, Massi D, Baroni G, Santucci M. Tumor lymphangiogenesis in head and neck squamous cell carcinoma: a morphometric study with clinical correlations. Cancer 2004;101:973–8.

[47] Maula S-M, Luukkaa M, Grénman R, Jackson D, Jalkanen S, Ristamaki R. Intratumoral lymphatics are essential for the metastatic spread and prognosis in squamous cell carcinomas of the head and neck region. Cancer Res 2003;63:1920–6.

[48] Sedivy R, Beck-Mannagetta J, Haverkampf C, Battistutti W, Honigschnabl S. Expression of vascular endothelial growth factor-C correlates with the lymphatic microvessel density and the nodal status in oral squamous cell cancer. J Oral Pathol Med 2003;32:455–60.

[49] Ohno F, Nakanishi H, Abe A, Seki Y, Kinoshita A, Hasegawa Y, et al. Regional difference in intratumoral lymphangiogenesis of oral squamous cell carcinomas evaluated by immunohistochemistry using D2-40 and podoplanin antibody: an analysis

in comparison with angiogenesis. J Oral Pathol Med 2007;36: 281—9.

[50] Van der Auwera I, Cao Y, Tille JC, Pepper MS, Jackson DG, Fox SB, et al. First international consensus on the methodology of lymphangiogenesis quantification in solid human tumours. Br J Cancer 2006;95:1611—25.

[51] Padera TP, Kadambi A, di Tomaso E, Carreira CM, Brown EB, Boucher Y, et al. Lymphatic metastasis in the absence of functional intratumor lymphatics. Science 2002;296:1883—6.

[52] Cairns RA, Khokha R, Hill RP. Molecular mechanisms of tumor invasion and metastasis: an integrated view. Curr Mol Med 2003;3:659—71.